

## Radio Emission From a $z = 10.3$ Black Hole in UHZ1

DANIEL J. WHALEN,<sup>1</sup> MUHAMMAD A. LATIF,<sup>2</sup> AND MAR MEZCUA<sup>3,4</sup>

<sup>1</sup>*Institute of Cosmology and Gravitation, Portsmouth University, Dennis Sciama Building, Portsmouth PO1 3FX*

<sup>2</sup>*Physics Department, College of Science, United Arab Emirates University, PO Box 15551, Al-Ain, UAE*

<sup>3</sup>*Institute of Space Sciences (ICE, CSIC), Campus UAB, Carrer de Magrans, 08193 Barcelona, Spain*

<sup>4</sup>*Institut d'Estudis Espacials de Catalunya (IEEC), Carrer Gran Capità, 08034 Barcelona, Spain*

### ABSTRACT

The recent discovery of a  $4 \times 10^7 M_{\odot}$  black hole (BH) in UHZ1 at  $z = 10.3$ , just 450 Myr after the big bang, suggests that the seeds of the first quasars may have been direct-collapse black holes (DCBHs) from the collapse of supermassive primordial stars at  $z \sim 20$ . This object was identified in *James Webb Space Telescope (JWST)* NIRcam and *Chandra* X-ray data, but recent studies suggest that radio emission from such a BH should also be visible to the Square Kilometer Array (SKA) and the next-generation Very Large Array (ngVLA). Here, we present estimates of radio flux for UHZ1 from 0.1 - 10 GHz, and find that SKA and ngVLA could detect it with integration times of 10 - 100 hr and just 1 - 10 hr, respectively. It may be possible to see this object with VLA now with longer integration times. The detection of radio emission from UHZ1 would be a first test of exciting new synergies between near infrared (NIR) and radio observatories that could open the era of  $z \sim 5 - 15$  quasar astronomy in the coming decade.

*Keywords:* quasars: supermassive black holes — black hole physics — early universe — dark ages, reionization, first stars — galaxies: formation — galaxies: high-redshift

### 1. INTRODUCTION

Nearly 300 quasars have now been discovered at  $z > 6$  (Fan et al. 2022), including nine at  $z > 7$  (Mortlock et al. 2011; Bañados et al. 2018; Yang et al. 2020; Wang et al. 2021). Both DCBHs and BHs forming from the collapse of normal Population III (Pop III) stars have been proposed as the seeds of these quasars. Pop III BHs are thought to form at  $z \sim 25$  with masses of a few tens to hundreds of solar masses and must accrete continuously at the Eddington limit or grow by super-Eddington accretion to reach  $10^9 M_{\odot}$  by  $z \sim 7$  (Volonteri et al. 2015; Inayoshi et al. 2016). This scenario is problematic because Pop III BHs are born in low densities that prevent rapid initial growth (e.g., Whalen et al. 2004; Latif et al. 2022a) and can be ejected from their host halos (and thus their fuel supply) during collapse (Whalen & Fryer 2012). If they begin to accrete later, they again drive gas out of their host halos because the shallow gravitational potential wells of their host halos, so they are restricted to fairly low duty cycles (Smith et al. 2018).

In contrast, DCBHs from the collapse of more rare  $10^4 - 10^5 M_{\odot}$  primordial stars (Hosokawa et al. 2013; Umeda et al. 2016; Woods et al. 2021; Herrington et al. 2023) at  $z \sim 20$  can grow at much higher rates at birth be-

cause Bondi-Hoyle accretion rates scale as  $M_{\text{BH}}^2$ . They also form in much higher ambient densities (e.g., Patrick et al. 2023) in more massive cosmological halos that retain gas even when it is heated by X-rays (Latif et al. 2021 - see Woods et al. 2019 for reviews). However, it has been thought until recently that DCBH formation required unusual or exotic environments that had little chance of coinciding with the rare, massive, low-shear halos needed to fuel the growth of the BH to  $10^9 M_{\odot}$  by  $z \sim 7$  (Tenneti et al. 2018; Lupi et al. 2021; Valentini et al. 2021). It is now known that the highly supersonic turbulence in these rare gas reservoirs can create DCBHs without the need for strong UV backgrounds, supersonic baryon streaming motions, or even atomic cooling (Latif et al. 2022b). Supermassive stars could be detected in the near infrared (NIR) at  $z \sim 8 - 14$  (Surace et al. 2018, 2019; Vikaeus et al. 2022; Nagele et al. 2023) and DCBHs could be detected at  $z \gtrsim 20$  in the NIR (Natarajan et al. 2017; Barrow et al. 2018; Whalen et al. 2020b) and at  $z \sim 8 - 10$  in the radio (Whalen et al. 2020a, 2021).

Observations of quasars at earlier stages of evolution, above  $z \sim 7$ , are clearly needed to distinguish between these formation pathways. One such object may have now been found, a  $4 \times 10^7 M_{\odot}$  BH at  $z = 10.3$  in UHZ1,

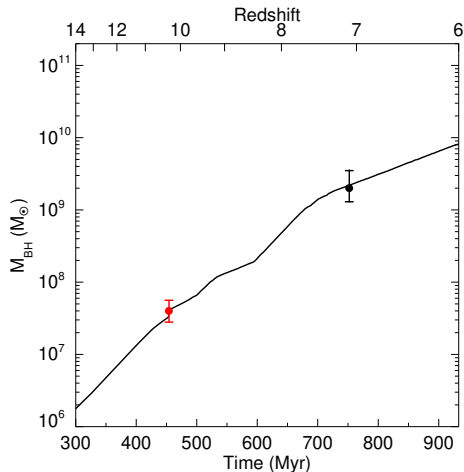


**Figure 1.** BH mass from Smidt et al. (2018), who modeled the formation of a quasar that is similar to J1120 (black), a  $1.35 \times 10^9 M_\odot$  BH at  $z = 7.1$ . UHZ1 (red), with a mass of  $4 \times 10^7 M_\odot$ , lies directly on this growth curve at  $z = 10.3$  and may be a  $z \sim 7$  quasar at an earlier stage of evolution.

which has been identified in *JWST* NIRcam and *Chandra* X-ray images (Bogdan et al. 2023). UHZ1 is a small galaxy that is gravitationally lensed by the Abel 2744 cluster (magnification  $\mu = 3.8$ ) and has a star formation rate (SFR) of  $4 M_\odot \text{ yr}^{-1}$ . Bogdan et al. (2023) suggest that the large mass of the BH at such early times favors a DCBH seed. This claim is corroborated by Smidt et al. (2018), who were the first to produce a quasar like J1120, a  $1.35 \times 10^9 M_\odot$  BH at  $z = 7.1$  (Mortlock et al. 2011), in a cosmological simulation. As shown in Figure 1, the BH in UHZ1 falls on the growth curve of that quasar. Recent calculations indicate that radio emission from this quasar should be visible to SKA and ngVLA at up to  $z \sim 14 - 16$  (Latif et al. 2023). Here, we estimate the radio flux expected from UHZ1 to determine if it could be detected and unambiguously confirm the presence of a BH there. In Section 2 we lay out our calculation of radio emission from the BH and H II regions and supernovae (SNe) in its host galaxy. We discuss prospects for its detection in current and future surveys in Section 3 and conclude in Section 4.

## 2. NUMERICAL METHOD

We calculate radio fluxes for the BH in UHZ1 from 0.1 - 10 GHz with fundamental planes (FPs) of BH accretion, which are empirical relationships between BH mass,  $M_{\text{BH}}$ , its nuclear X-ray luminosity at 2 - 10 keV,  $L_X$ , and its nuclear radio luminosity at 5 GHz,  $L_R$  (Merloni et al. 2003). FPs cover six orders of magnitude in

BH mass down to intermediate-mass black holes ( $< 10^5 M_\odot$ ; Gültekin et al. 2014).

### 2.1. BH Radio Flux

To find the BH radio flux in a given band in the Earth frame we first use an FP to calculate  $L_R$  in the source frame, which depends on  $M_{\text{BH}}$  and  $L_X$ . We find  $L_X$  from  $L_{\text{bol}}$ , the bolometric luminosity of the BH, with Equation 21 of Marconi et al. (2004),

$$\log \left( \frac{L_{\text{bol}}}{L_X} \right) = 1.54 + 0.24\mathcal{L} + 0.012\mathcal{L}^2 - 0.0015\mathcal{L}^3, \quad (1)$$

where  $L_{\text{bol}}$  is in units of solar luminosity,  $\mathcal{L} = \log L_{\text{bol}} - 12$ , and we take  $L_{\text{bol}} = 5 \times 10^{45} \text{ erg s}^{-1}$  from Bogdan et al. (2023).  $L_R$  can then be determined from  $L_X$  from the FP,

$$\log L_R(\text{erg s}^{-1}) = \alpha \log L_X(\text{erg s}^{-1}) + \beta \log M_{\text{BH}}(M_\odot) + \gamma, \quad (2)$$

where  $\alpha$ ,  $\beta$  and  $\gamma$  are for FPs from Merloni et al. (2003, MER03), Körding et al. (2006, KOR06), Gültekin et al. (2009, GUL09), Plotkin et al. (2012, PLT12), and Bonchi et al. (2013, BON13) and are listed in Table 1 of Latif et al. (2023). We also include the FP of Equation 19 in Gültekin et al. (2019, GUL19), which has a slightly different form:

$$R = -0.62 + 0.70 X + 0.74 \mu, \quad (3)$$

where  $R = \log(L_R/10^{38} \text{ erg/s})$ ,  $X = \log(L_X/10^{40} \text{ erg/s})$  and  $\mu = \log(M_{\text{BH}}/10^8 M_\odot)$ .

Radio flux from a supermassive black hole (SMBH) that is cosmologically redshifted into a given observer band today does not originate from 5 GHz in the source frame at high redshifts, so we calculate it from  $L_R = \nu L_\nu$  assuming that the spectral luminosity  $L_\nu \propto \nu^{-\alpha}$ . We consider  $\alpha = 0.7$  and  $0.3$  to bracket a reasonable range of spectral profiles (Condon et al. 2002; Gloude-mans et al. 2021). The spectral flux at  $\nu$  in the Earth frame is then calculated from the spectral luminosity at  $\nu'$  in the rest frame from

$$F_\nu = \frac{L_{\nu'}(1+z)}{4\pi d_L^2}, \quad (4)$$

where  $\nu' = (1+z)\nu$  and  $d_L$  is the luminosity distance. In calculating  $d_L$  we assume second-year *Planck* cosmological parameters:  $\Omega_M = 0.308$ ,  $\Omega_\Lambda = 0.691$ ,  $\Omega_b h^2 = 0.0223$ ,  $\sigma_8 = 0.816$ ,  $h = 0.677$  and  $n = 0.968$  (Planck Collaboration et al. 2016).

### 2.2. Supernova Radio Flux

Synchrotron emission from young SN remnants in the host galaxy could contribute to the total radio emission

from UHZ1. Condon (1992) estimate the non-thermal radio flux from SNe in star-forming galaxies today to be

$$\left(\frac{L_N}{\text{W Hz}^{-1}}\right) \sim 4.4 \times 10^{34} \left(\frac{\nu}{\text{GHz}}\right)^{-\beta} \left[\frac{\text{SFR}(M > 5 M_\odot)}{M_\odot \text{ yr}^{-1}}\right], \quad (5)$$

where  $\beta \sim 0.8$  is the spectral index and we set  $\text{SFR} = 4 M_\odot \text{ yr}^{-1}$  from Bogdan et al. (2023) for simplicity because the stellar IMF is unknown. Equation 5 may overestimate the SN flux from UHZ1 because core-collapse SNe (Joggerst et al. 2010; Latif et al. 2022a) only produce nJy radio fluxes (Meiksin & Whalen 2013) in the diffuse H II regions of high-redshift halos (Whalen et al. 2004, 2008). Since we also assume that SF only produces stars  $> 5 M_\odot$ , this flux should be taken to be an upper limit.

### 2.3. H II Region Radio Emission

Thermal bremsstrahlung in H II regions due to active SF also produces continuum radio flux whose spectral density can be calculated from the ionizing photon emission rate in the H II region,  $Q_{\text{Lyc}}$ :

$$L_\nu \lesssim \left(\frac{Q_{\text{Lyc}}}{6.3 \times 10^{52} \text{ s}^{-1}}\right) \left(\frac{T_e}{10^4 \text{ K}}\right)^{0.45} \left(\frac{\nu}{\text{GHz}}\right)^{-0.1} \quad (6)$$

in units of  $10^{20} \text{ W Hz}^{-1}$  (Condon 1992), where  $Q_{\text{Lyc}} = \text{SFR} (M_\odot \text{ yr}^{-1}) / 1.0 \times 10^{-53}$  (Kennicutt 1998). We again take  $\text{SFR} = 4$  and  $T_e = 10^4 \text{ K}$ .

## 3. RESULTS AND DISCUSSION

We show radio fluxes for UHZ1 for  $\alpha = 0.3$  and 0.7 for all six FPs in Figure 2 along with the H II region and SN fluxes for its host galaxy. They vary from 1.3 - 32  $\mu\text{Jy}$  at 100 MHz to 0.065 - 1.3  $\mu\text{Jy}$  at 10 GHz for  $\alpha = 0.7$  and from 0.9 - 20  $\mu\text{Jy}$  at 100 MHz to 0.23 - 1.1  $\mu\text{Jy}$  at 10 GHz for  $\alpha = 0.3$ . As expected, the highest fluxes are at the lowest frequencies, and they fall by a factor of a few to an order of magnitude by 10 GHz. Most of the FP fluxes for  $\alpha = 0.3$  could be detected with 10 hr integration times by the SKA (see Table 3 of Braun et al. 2019) and virtually all of them could be found with 100 hr pointings, as shown by the detection bars in Figure 2.

The ngVLA could detect the smallest of the fluxes with just 1 hr integration times over its bandwidth (Plotkin & Reines 2018). For  $\alpha = 0.7$ , the smallest of the radio fluxes could be detected with a 10 hr pointing by ngVLA and 100 hr integration times with SKA. However, the top two FP fluxes could be found by just 1 hr integration times by SKA for both  $\alpha$ . The H II region flux is only  $\sim 20 \text{ nJy}$  but the SN flux comes within a factor of 2 of the lowest BH fluxes at 0.1 GHz. It

falls steeply thereafter and is at most 1% - 10% of even the lowest BH fluxes above 1 GHz. Consequently, any detection of radio emission from UHZ1 except perhaps at the lowest frequencies would unambiguously confirm the existence of a BH there.

UHZ1 does not appear in recent VLA or upgraded Giant Metrewave Radio Telescope (uGMRT) observations of Abel 2744 at the 7  $\mu\text{Jy}/\text{beam}$  RMS noise level in the VLA *L*-band (1 - 2 GHz), at 5  $\mu\text{Jy}$  in the VLA *S*-band (2 - 4 GHz), at 41  $\mu\text{Jy}$  in uGMRT band 3 (300 - 500 MHz), or at 7  $\mu\text{Jy}$  in uGMRT band 4 (550 - 950 MHz; see Table 3 of Rajpurohit et al. 2021). Figure 2 shows that uGMRT therefore rules out the GUL09 and GUL19 FPs for  $\alpha = 0.3$  but only GUL09 for  $\alpha = 0.7$ . All the FPs are consistent with the VLA data because they fall below its noise limits.

## 4. CONCLUSION

Our estimates show that radio emission from UHZ1 at  $z = 10.3$  would be easily detected by SKA and ngVLA in the coming decade, but with sufficient integration times it may be possible to detect with VLA now. Radio measurements of UHZ1 might also detect features of the BH that may not appear in the NIR or X-rays, such as jets (whose fluxes we do not consider here). The angular diameter of UHZ1 is  $\sim 0.25''$  but SKA will reach angular resolutions of 0.08'' and 0.04'' at 6.5 GHz and 10 GHz, respectively, and could partially resolve radio structure originating from the host galaxy. It is not clear if the BH in UHZ1 would have a jet because it is assumed to be accreting at about the Eddington limit and jets have mostly been observed at  $L_{\text{bol}} \lesssim 0.01 L_{\text{Edd}}$  and  $L_{\text{bol}} \gtrsim L_{\text{Edd}}$ . If a jet did form, the cosmic microwave background might quench its emission (Ghisellini et al. 2014; Fabian et al. 2014). Nevertheless, compact jets have been observed from high-redshift quasars on scales of a kpc or less in one or two cases (Momjian et al. 2018; Connor et al. 2021) and could be resolved by SKA or ngVLA measurements.

Latif et al. (2023) found that SKA and ngVLA could detect BHs like UHZ1 at earlier stages of evolution at lower masses and higher redshifts, in principle up to  $z \sim 14 - 16$ , but in targeted searches rather than blind surveys because the numbers of massive BHs at these redshifts are so small. UHZ1 is an excellent such target, not only to complement prior NIR and X-ray measurements but to develop radio followups on photometric detections of SMBH candidates by *Euclid* and the *Roman Space Telescope (RST)* at  $z \lesssim 15$  in the coming decade. The discovery of radio emission from UHZ1 would be the first test of potential synergies between NIR surveys and

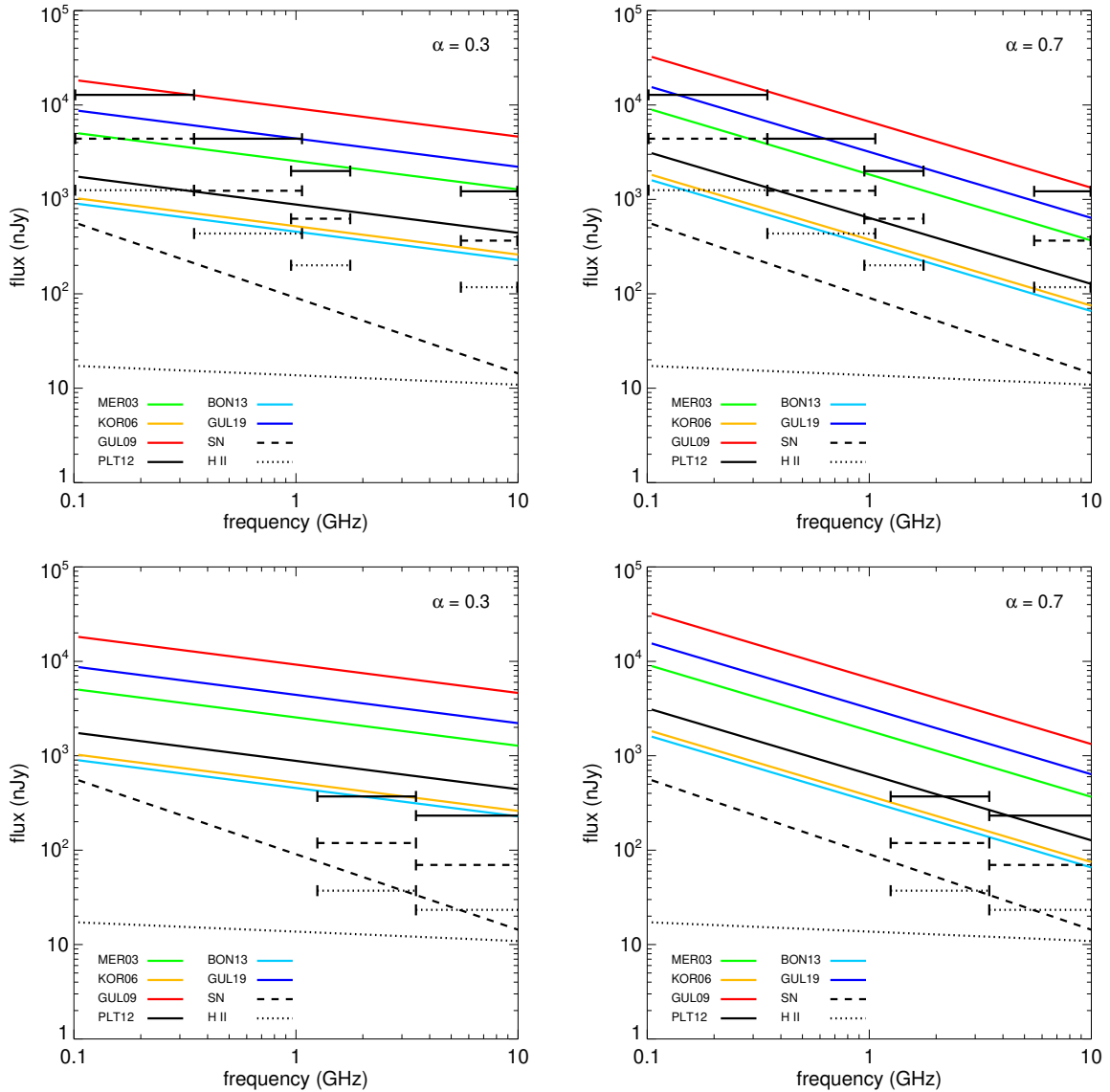


**Figure 2.** Radio fluxes for the BH in UHZ1 at 0.1 - 10 GHz. The horizontal bars are detection limits as explained below. Left panels:  $\alpha = 0.3$ . Right panels:  $\alpha = 0.7$ . Top row: horizontal lines indicate SKA detection limits for 1 hr (solid), 10 hr (dashed) and 100 hr (dotted) integration times. Bottom row: BH fluxes with ngVLA detection limits for 1 hr (solid), 10 hr (dashed) and 100 hr (dotted) integration times. All fluxes have been boosted by the lensing factor  $\mu = 3.81$  from Bogdan et al. (2023).

radio observations in detections of  $z \sim 5 - 15$  quasars in the coming decade.

#### ACKNOWLEDGMENTS

The authors thank Akos Bogdan, David Bacon and Matt Jarvis for helpful discussions. MAL thanks the UAEU for funding via UPAR grants No. 31S390 and 12S111. This work was also supported by the program Unidad de Excelencia María de Maeztu CEX2020-001058-M.

#### REFERENCES

Bañados, E., et al. 2018, *Nature*, 553, 473

Barrow, K. S. S., Aykutaalp, A., & Wise, J. H. 2018, *Nature Astronomy*, 2, 987

- Bogdan, A., et al. 2023, arXiv:2305.15458
- Bonchi, A., La Franca, F., Melini, G., Bongiorno, A., & Fiore, F. 2013, MNRAS, 429, 1970
- Braun, R., Bonaldi, A., Bourke, T., Keane, E., & Wagg, J. 2019, arXiv:1912.12699
- Condon, J. J. 1992, ARA&A, 30, 575
- Condon, J. J., Cotton, W. D., & Broderick, J. J. 2002, AJ, 124, 675
- Connor, T., et al. 2021, ApJ, 911, 120
- Fabian, A. C., Walker, S. A., Celotti, A., Ghisellini, G., Mocz, P., Blundell, K. M., & McMahon, R. G. 2014, MNRAS, 442, L81
- Fan, X., Banados, E., & Simcoe, R. A. 2022, arXiv e-prints, arXiv:2212.06907
- Ghisellini, G., Celotti, A., Tavecchio, F., Haardt, F., & Sbarrato, T. 2014, MNRAS, 438, 2694
- Gludemans, A. J., et al. 2021, A&A, 656, A137
- Gültekin, K., Cackett, E. M., King, A. L., Miller, J. M., & Pinkney, J. 2014, ApJL, 788, L22
- Gültekin, K., Cackett, E. M., Miller, J. M., Di Matteo, T., Markoff, S., & Richstone, D. O. 2009, ApJ, 706, 404
- Gültekin, K., King, A. L., Cackett, E. M., Nyland, K., Miller, J. M., Di Matteo, T., Markoff, S., & Rupen, M. P. 2019, ApJ, 871, 80
- Herrington, N. P., Whalen, D. J., & Woods, T. E. 2023, MNRAS, 521, 463
- Hosokawa, T., Yorke, H. W., Inayoshi, K., Omukai, K., & Yoshida, N. 2013, ApJ, 778, 178
- Inayoshi, K., Haiman, Z., & Ostriker, J. P. 2016, MNRAS, 459, 3738
- Joggerst, C. C., Almgren, A., Bell, J., Heger, A., Whalen, D., & Woosley, S. E. 2010, ApJ, 709, 11
- Kennicutt, Robert C., J. 1998, ARA&A, 36, 189
- Körding, E., Falcke, H., & Corbel, S. 2006, A&A, 456, 439
- Latif, M. A., Khochfar, S., Schleicher, D., & Whalen, D. J. 2021, MNRAS, 508, 1756
- Latif, M. A., Whalen, D., & Khochfar, S. 2022a, ApJ, 925, 28
- Latif, M. A., Whalen, D. J., Khochfar, S., Herrington, N. P., & Woods, T. E. 2022b, Nature, 607, 48
- Latif, M. A., Whalen, D. J., & Mezcuca, M. 2023, arXiv:2304.12333
- Lupi, A., Haiman, Z., & Volonteri, M. 2021, MNRAS, 503, 5046
- Marconi, A., Risaliti, G., Gilli, R., Hunt, L. K., Maiolino, R., & Salvati, M. 2004, MNRAS, 351, 169
- Meiksin, A., & Whalen, D. J. 2013, MNRAS, 430, 2854
- Merloni, A., Heinz, S., & di Matteo, T. 2003, MNRAS, 345, 1057
- Momjian, E., Carilli, C. L., Bañados, E., Walter, F., & Venemans, B. P. 2018, ApJ, 861, 86
- Mortlock, D. J., et al. 2011, Nature, 474, 616
- Nagele, C., Umeda, H., Takahashi, K., & Maeda, K. 2023, MNRAS, 520, L72
- Natarajan, P., Pacucci, F., Ferrara, A., Agarwal, B., Ricarte, A., Zackrisson, E., & Cappelluti, N. 2017, ApJ, 838, 117
- Patrick, S. J., Whalen, D. J., Latif, M. A., & Elford, J. S. 2023, MNRAS, 522, 3795
- Planck Collaboration et al. 2016, A&A, 594, A13
- Plotkin, R. M., Markoff, S., Kelly, B. C., Körding, E., & Anderson, S. F. 2012, MNRAS, 419, 267
- Plotkin, R. M., & Reines, A. E. 2018, arXiv:1810.06814, arXiv:1810.06814
- Rajpurohit, K., et al. 2021, A&A, 654, A41
- Smidt, J., Whalen, D. J., Johnson, J. L., Surace, M., & Li, H. 2018, ApJ, 865, 126
- Smith, B. D., Regan, J. A., Downes, T. P., Norman, M. L., O'Shea, B. W., & Wise, J. H. 2018, MNRAS, 480, 3762
- Surace, M., Zackrisson, E., Whalen, D. J., Hartwig, T., Glover, S. C. O., Woods, T. E., Heger, A., & Glover, S. C. O. 2019, MNRAS, 488, 3995
- Surace, M., et al. 2018, ApJL, 869, L39
- Tenneti, A., Di Matteo, T., Croft, R., Garcia, T., & Feng, Y. 2018, MNRAS, 474, 597
- Umeda, H., Hosokawa, T., Omukai, K., & Yoshida, N. 2016, ApJL, 830, L34
- Valentini, M., Gallerani, S., & Ferrara, A. 2021, MNRAS, 507, 1
- Vikaeus, A., Whalen, D. J., & Zackrisson, E. 2022, ApJL, 933, L8
- Volonteri, M., Silk, J., & Dubus, G. 2015, ApJ, 804, 148
- Wang, F., et al. 2021, ApJL, 907, L1
- Whalen, D., Abel, T., & Norman, M. L. 2004, ApJ, 610, 14
- Whalen, D., van Veelen, B., O'Shea, B. W., & Norman, M. L. 2008, ApJ, 682, 49
- Whalen, D. J., & Fryer, C. L. 2012, ApJL, 756, L19
- Whalen, D. J., Mezcuca, M., Meiksin, A., Hartwig, T., & Latif, M. A. 2020a, ApJL, 896, L45
- Whalen, D. J., Mezcuca, M., Patrick, S. J., Meiksin, A., & Latif, M. A. 2021, ApJL, 922, L39
- Whalen, D. J., Surace, M., Bernhardt, C., Zackrisson, E., Pacucci, F., Ziegler, B., & Hirschmann, M. 2020b, ApJL, 897, L16
- Woods, T. E., Patrick, S., Elford, J. S., Whalen, D. J., & Heger, A. 2021, ApJ, 915, 110
- Woods, T. E., et al. 2019, Publications of the Astronomical Society of Australia, 36, e027
- Yang, J., et al. 2020, ApJL, 897, L14